Revision of the Crystal Structure of the Orthorhombic Polymorph of Oxyma: On the Importance of π−Hole Interactions and Their Interplay with H−Bonds

Article *in* Crystals · June 2022

DOI: 10.3390/cryst12060823

5 authors, including:

Rafa Barbas
University of Barcelona
49 PUBLICATIONS **764** CITATIONS
SEE PROFILE

Dafne de Sande López
University of Barcelona
11 PUBLICATIONS **55** CITATIONS
SEE PROFILE

Rafel Prohens
University of Barcelona
107 PUBLICATIONS **2,200** CITATIONS
SEE PROFILE

Antonio Frontera
University of the Balearic Islands
892 PUBLICATIONS **22,190** CITATIONS
SEE PROFILE

crystals

MDPI

Article

Revision of the Crystal Structure of the Orthorhombic Polymorph of Oxyma: On the Importance of π–Hole Interactions and Their Interplay with H–Bonds

Rafael Barbas [1], Dafne de Sande [1], Mercè Font-Bardia [2], Rafel Prohens [1,*] and Antonio Frontera [3,*]

[1] Unitat de Polimorfisme i Calorimetria, Centres Científics i Tecnològics, Universitat de Barcelona, Baldiri Reixac 10, 08028 Barcelona, Spain; rafa@ccit.ub.edu (R.B.); dafne@ccit.ub.edu (D.d.S.)
[2] Unitat de Difracció de Raigs X, Centres Científics i Tecnològics, Universitat de Barcelona, 08028 Barcelona, Spain; mercef@ccit.ub.edu
[3] Departament de Química, Universitat de les Illes Balears, Crta. de Valldemossa, km 7.5, 07122 Palma (Baleares), Spain
* Correspondence: rafel@ccit.ub.edu (R.P.); toni.frontera@uib.es (A.F.)

Abstract: In this work the crystal structure of the previously described orthorhombic polymorph of the coupling reagent Oxyma has been revised, corrected now as centrosymmetric and analyzed by means of DFT calculations. In the solid state the structure forms a network of H-bonds and self–assembled dimers that are held together by the formation of N···C π–hole interactions involving the C-atom of the imino group. The H-bonding and π–hole interactions observed in the solid state were rationalized using molecular electrostatic potential (MEP) surfaces, focusing on the H-bond donor-acceptor groups and the π-hole observed above and below the molecular plane. The interactions and their interplay have been characterized by using two methodologies based on the topology of the electron density, which are the quantum theory of "atom-in-molecules" (QTAIM) and the noncovalent interaction plot (NCIplot).

Keywords: hydrogen bonding; π–hole interactions; crystal engineering; supramolecular chemistry; DFT calculations

Citation: Barbas, R.; de Sande, D.; Font-Bardia, M.; Prohens, R.; Frontera, A. Revision of the Crystal Structure of the Orthorhombic Polymorph of Oxyma: On the Importance of π–Hole Interactions and Their Interplay with H–Bonds. *Crystals* **2022**, *12*, 823. https://doi.org/10.3390/cryst12060823

Academic Editor: Jesús Sanmartín-Matalobos

Received: 21 May 2022
Accepted: 8 June 2022
Published: 10 June 2022

1. Introduction

The hydrogen bonding (HB) [1–3] is used to refer to any attractive interaction between a hydrogen atom of a molecule or molecular fragment and an atom or group of atoms acting as electron donors. Since its establishment as noncovalent non-covalent force a century ago, hydrogen bonding is under continuous study and endlessness applied in chemistry, biology, and materials [1–3]. Other forces like π–hole interactions involving elements of the p-block as electron acceptors (playing the role of the H-atom) are gaining attention among the scientific com-munity, and specially in crystal engineering and supramolecular chemistry [4]. Depletion of electron density usually happens on the extension of covalent bonds like H-bonds and σ-hole interactions. However, depletion can also occur above planar groups as well, as for example above a carbonyl or phenyl group because of their location and association with π-electronic systems. These regions of density depletion and positive electrostatic potential are called π-holes, exemplified by tricoordinated triel atoms, where the typical π–hole is located above and below the center of the planar triangle, where the triel atom is positioned [4–9]. Other common π-hole is that situated above the C atom of a carbonyl group [10]. In fact, π-hole interactions involving C-atoms are important in protein structures [11,12].

Ethyl 2-cyano-2-(hydroxyimino)acetate (Oxyma), commercialized as OxymaPure® trademark [13] (Figure 1), is a compound used as an additive for peptide synthesis in combination with carbodiimides with high performance in terms of suppression of racemization and of coupling efficiency [14]. It shows a remarkable lower risk of explosion than

other Oxyma-based coupling reagents [15,16] which converts Oxyma in one of the most commonly coupling agent used in Solid Phase Peptide Synthesis [14].

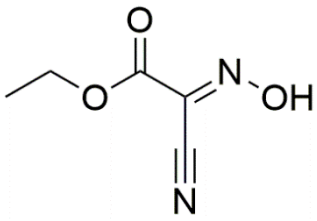

Figure 1. Chemical structure of Oxyma.

In this manuscript, the X-ray structure of the orthorhombic polymorph of Oxyma is revisited and analyzed. It should be mentioned that some of us were involved in the analysis of the thermal risk properties of Oxyma [14] and during that study good quality single crystals were obtained. Since the orthorhombic crystallographic cell determined by SCXRD matched the one deposited in the CCDC with deposition number 148,718 we did not solve its crystal structure. Some years after the crystal structure of a new low temperature monoclinic polymorph was reported [17] and it is available in the CCDC with deposition number 1,473,516. In that work the authors mentioned also the existence of the orthorhombic polymorph, which has motivated us to revisit the polymorphism of this important industrial compound. Thus, we reanalyzed our original raw data and compared to the available orthorhombic structure, a cif file containing only atomic coordinates. Moreover, we have focused this manuscript on the existence and relevance of π-hole interactions involving the C-atom of the ester group and their interplay with strong H-bonds. This type of π-holes involving esters have been scarcely described and exploited in the literature. In addition, the crystal structure of Oxyma further discloses the co-existence of several hydrogen bonds (OH···O and OH···N) that contribute to the formation of infinite 1D assemblies. These interactions have been characterized energetically using DFT calculations, the quantum theory of atoms-in-molecules (QTAIM), molecular electrostatic potential (MEP) surfaces and the noncovalent interaction plot (NCIPlot) computational tools.

2. Materials, Experimental and Theoretical Methods

2.1. Materials

Oxyma was used from commercial sources (Sigma-Aldrich, St. Louis, MO, USA).

2.2. Synthesis of the Single Crystals

Single crystals of Oxyma were obtained by recrystallization in acetone as follows: Oxyma (20 mg, 0.141 mmol) was dissolved in acetone (0.6 mL) at 60 °C. Then, the solution was cooled down to 25 °C and kept sealed at room temperature. Single crystals were observed and collected after 24 h.

2.3. Single Crystal X-ray Diffraction

A colorless prism-like specimen of Oxyma ($C_5H_6N_2O_3$) with approximate dimensions 0.100 mm × 0.100 mm × 0.200 mm, was used for the X-ray crystallographic analysis. The X-ray intensity data were measured on a MAR346 system equipped with a graphite monochromator and a Mo fine-focus sealed tube (λ = 0.71073 Å). The frames were integrated with the Bruker SAINT software package(Madison, WI, USA) using a narrow-frame algorithm. The integration of the data using an orthorhombic unit cell yielded a total of 1036 reflections to a maximum θ angle of 33.02° (0.65 Å resolution), of which 1036 were independent (average redundancy 1.000, completeness = 72.1%, $R_{in}t$ = 6.04%, R_{sig} = 0.26%) and 1023 (98.75%) were greater than 2σ(F2). The final cell constants of a = 7.997(7) Å, b = 6.512(5) Å, c = 13.622(8) Å, volume = 709.4(11) $Å^3$, are based upon the refinement of the XYZ-centroids of reflections above 20 σ(I). Data were corrected for absorption effects using the empirical method (SADABS) [18]. The calculated minimum and maximum

transmission coefficients (based on crystal size) are 0.9700 and 0.9900. The structure was solved and refined using the Bruker SHELXTL Software Package(Madison, Wisconsin, USA) [19], using the space group Pnma, with Z = 4 for the formula unit, $C_5H_6N_2O_3$. The final anisotropic full-matrix least-squares refinement on F^2 with 67 variables converged at R_1 = 7.32%, for the observed data and wR_2 = 12.11% for all data. The goodness-of-fit was 1.394. The largest peak in the final difference electron density synthesis was 0.168 e/Å^3 and the largest hole was −0.145 e/Å^3 with an RMS deviation of 0.035 e-/Å^3. On the basis of the final model, the calculated density was 1.331 g/cm^3 and F(000), 296 e.

2.4. Computational Details

The calculations of the non-covalent interactions were carried out using the Gaussian-16 [20] and the PBE0-D3/def2-TZVP level of theory [21,22]. To evaluate the interactions in the solid state, the crystallographic coordinates were used. The binding energies were computed by calculating the difference between the energies of isolated monomers and their assembly. The binding energies were evaluated with correction for the basis set superposition error (BSSE) by using the Boys–Bernardi method [23]. The Bader's "Atoms in molecules" theory (QTAIM) [24] was used to study the π-hole and H-bonding interactions discussed herein by means of the AIMAll calculation package [25]. The molecular electrostatic potential surfaces (isosurface 0.001 a.u.) were computed using the Gaussian-16 software (Gaussian Inc., Wallingford, CT, USA) [20].

In order to assess the nature of interactions in terms of being attractive or repulsive and revealed them in real space, we have used NCIPLOT index, which is a method for plotting non-covalent interaction regions [26], based on the NCI (Non-Covalent Interactions) visualization index derived from the electronic density [27]. The reduced density gradient (RDG), coming from the density and its first derivative, is plotted as a function of the density (mapped as isosurfaces) over the molecule of interest. The sign of the second Hessian eigenvalue times the electron density [i.e., sign(λ_2) ρ in atomic units] enables the identification of attractive/stabilizing (blue-green coloured isosurfaces) or repulsive (yellow-red coloured isosurfaces) interactions using 3D-Plots. For the plots shown in the next section the NCIplot index parameters are: RGD isosurface = 0.5; ρ cut off = 0.04 a.u.; color range: -0.04 a.u. $\leq$ sign(λ_2) ρ $\leq$ 0.04 a.u.

3. Results and Discussion

3.1. Revision of the Crystal Structure of the Orthorhombic Polymorph of Oxyma

A careful evaluation of the X-ray data revealed that the structure should be centrosymmetric with *Pnma* space group instead of the previously reported [28] non centrosymmetryc *Pmc*21 space group. Table S1 of ESI contains the most relevant crystallographic parameters of the new solution and Section 4 of ESI contains the checkcif details of the uncorrected structure. Table S2 of ESI gathers the H-bonding details.

Our revised structure has been now deposited in the CCDC with 2,173,714 number. In addition, we have analyzed the differences between both polymorphs (see Table S3, ESI), which are essentially crystallographic but negligible from a supramolecular chemistry point of view, since the intermolecular interactions are exactly the same in both polymorphs (they are analyzed in detail in Section 3.2). They can be considered conformational polymorphs with the most relevant difference in the torsion angle between the ethoxy and the hydroxylamine groups, being perfectly co-planar in the orthorhombic polymorph (N1-C4-C3-O1 torsion angle 180.0°) but slightly bent in the monoclinic one (torsion angle 176.5°). The second relevant difference is the presence in the orthorhombic form of static discrete disorder in the ethoxy group as a consequence of the mirror plane perpendicular to [010] (Figure 2), which is absent in the monoclinic form. The monoclinic polymorph was solved at 120 K while the orthorhombic form has been solved at 293 K, which can explain the presence of disorder in a region which is held by weak interactions. In the Supplementary file, further characterization of this polymorph is provided, including the differential scanning calorimetry (DSC, Figure S1) and thermogravimetric analysis (TGA,

Figure S2). Finally, aiming to complete the structural analysis of Oxyma a comprehensive DFT study was conducted as follows.

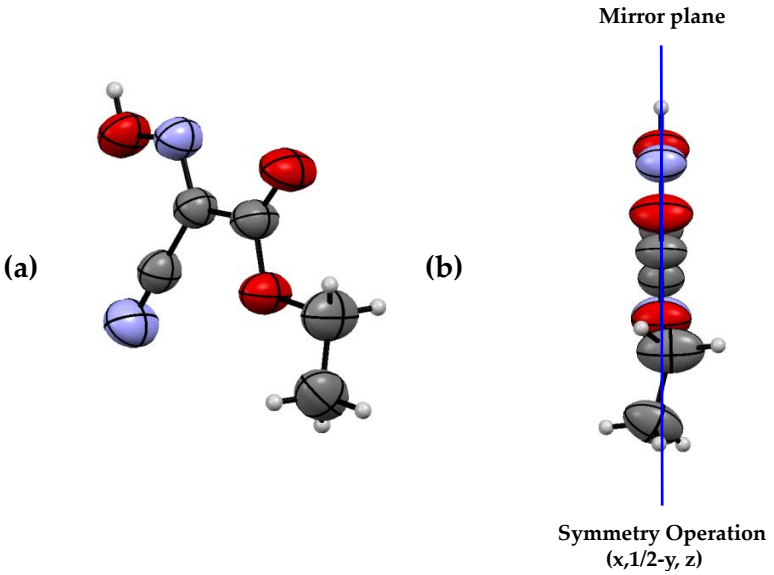

Figure 2. (**a**) ORTEP representation of the orthorhombic polymorph asymmetric unit, (**b**) mirror plane perpendicular to [010].

3.2. DFT Calculations

The DFT study is basically focused on the analysis of the interactions observed in the crystal structure of the orthorhombic polymorph of Oxyma but it can be essentially extended to the monoclinic one. Figure 3a shows a partial view of the X-ray structure of the where the formation of OH···O=C H-bonds propagates the monomer into 1D infinite chains (1.88 Å, H···O distance, see Table S2 for further geometrical details). In addition, Figure 3b shows the formation 1D columns with an antiparallel arrangement of the Oxyma molecules. A more detailed representation in shown Figure 3b (right) using a dimer extracted from the infinite assembly. It evidences the formation of two symmetrically equivalent N···C contacts (C···N distance: 3.279 Å) where the N-atom of the cyano group is located precisely over the C-atom of the carbonyl group.

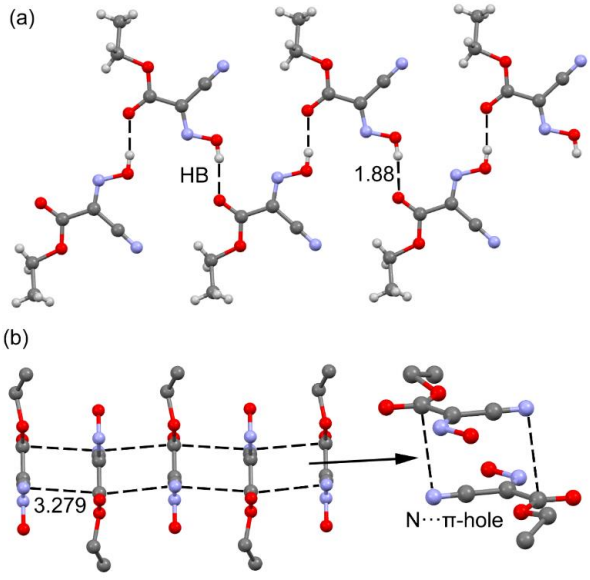

Figure 3. Partial view of the X-ray structure of Oxyma with indication of the H-bonds (**a**) and π–hole interactions (**b**). Distances in Å. The H-atoms have been omitted in (**b**) for clarity.

The MEP surface of Oxyma was initially computed (see Figure 4) to investigate the most electron rich and electron poor regions. We have used both a monomeric form and also an H-bonded trimeric assembly in order to investigate how the formation of the H-bonds affects the MEP values over the C-atom of the carbonyl group. In the monomer (Figure 4a), the MEP minimum is located at the O-atom of the carbonyl group (–34.5 kcal/mol) followed by that at the N-atom of the cyano group (−33.5 kcal/mol). The maximum MEP is located at the OH group (+65.2 kcal/mol) as expected. Therefore, the H-bonds described in Figure 3a are the most favored interactions considering only electrostatic effects. Moreover, the MEP over the sp^2-hybridized C-atoms is positive (+18.8 kcal/mol) thus revealing the existence of a π-hole in this molecule that is adequate for interacting with electron rich atoms. The π-hole depth of the isolated molecule is likely modulated by the formation of the strong H-bonds. To analyze this effect, we have computed the MEP surface of a trimeric specie as model of the polymeric chain and focus on the central molecule, that establishes one H-bond as donor and one as acceptor. These H-bonds are expected to have an opposite effect upon the MEP over the C-atom. The MEP of the trimer reveals that the π-hole becomes more positive, thus increasing its ability to interact with Lewis bases, and also increases the nucleophilicity of nitrile's N-atom since the MEP becomes more negative. This MEP analysis anticipates a favorable cooperativity between the H-bonds and N···π-hole interactions.

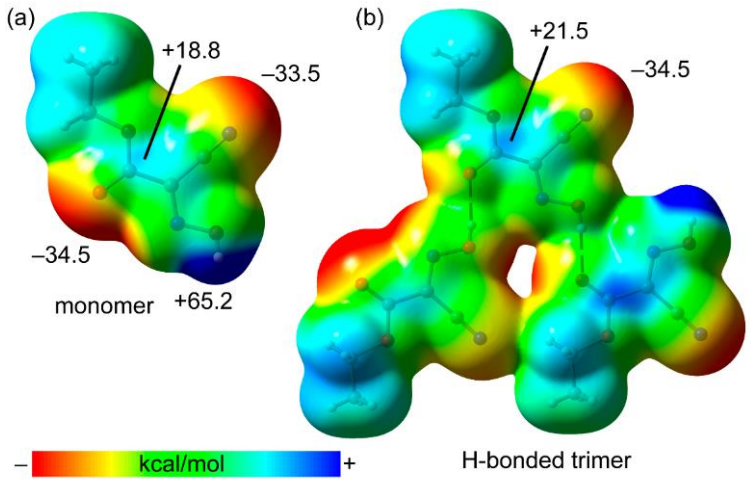

Figure 4. MEP surfaces of a monomer (**a**) and trimer (**b**) of Oxyma at the PBE0-D3/def2-TZVP level of theory (isosurface 0.001 a.u.). The energies at selected points of the surface are given in kcal/mol.

Figure 5a shows the combined QTAIM/NCIPlot analysis of the H-bonded trimer, evidencing that each H-bond is characterized by a bond critical point (CP, red sphere) and bond path interconnecting the H and O, N-atoms. Interestingly, it discloses the existence of an additional CH···N contact involving one H-atom of the ethyl group and the N-atom of the cyano group. The OH··O interactions are also characterized by blue (strong attractive) NCIplot isosurfaces coincident to the location of the bond CPs. The CH···O interaction is characterized by a green NCIplot isosurface indicating that this interaction is weaker. The total binding energy of this trimer is $\Delta E_1 = -13.1$ kcal/mol, thus confirming the importance of these H-bonds governing the solid state architecture of Oxyma. To compare the strength of the different H-bonds, the simple and reliable methodology recently proposed by Emaniam et al. [29] has been used. In particular, to quantitatively evaluate the hydrogen bond strength (ΔE, in kcal/mol) it uses the electron density (ρ in a.u.) at the BCPs and the equation $\Delta E = -233.1 \times \rho + 0.7$. The values are indicated in Figure 5a (in red) revealing that the OH···O interactions are stronger (−5.6 kcal/mol) than the CH···N (−1.2 kcal/mol) in line with the NCIplot RDG isosurfaces. To total formation energy of the assembly ($\Delta E_1 = -13.1$ kcal/mol) is similar to the sum of the individual HB energies (−12.4 kcal/mol), thus giving reliability to the energy predictor [29]. The small difference

(0.7 kcal/mol) is likely due to the contribution of the attractive interaction between the N-atom of the oxime group and the hydroxyl H-atom, as corroborated by the green isosurface located between both atoms (see small arrows in Figure 5a), although such small difference is within the accuracy of the DFT method. Figure 5b shows the QTAIM analysis of the π-hole dimer, showing two symmetrically equivalent bond CPs and bond paths connecting the N-atoms to the C-atoms, thus corroborating the existence of the double N···π-hole interactions. The interaction is further characterized by an extended green NCIplot isosurface, disclosing the attractive nature of the interaction. The dimerization energy is $\Delta E_2 = -5.2$ kcal/mol, thus suggesting that these contacts are moderately strong. The QTAIM/NCIPlot analysis discloses the existence of CH···O contacts that are very weak (−0.3 kcal/mol), thus confirming that the formation of this dimer is dominated by the π-hole interactions.

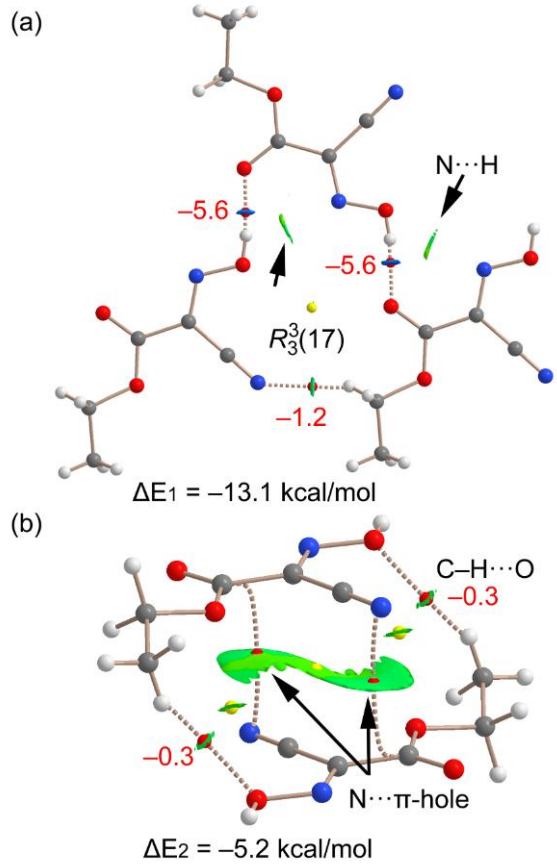

Figure 5. QTAIM/NCIPlot analysis of the H-bond trimer (**a**) and π-hole dimer of Oxyma (**b**). The bond CPs are represented as red spheres and bond paths as dashed lines. Only intermolecular CPs bond paths and RDG isosurfaces are shown.

In order to analyze if the π-hole interaction is reinforced by the presence of the H-bond, we have computed the tetramer shown in Figure 6 where the formation energy ($\Delta E_3 = -5.8$ kcal/mol) has been computed as a dimer, where the OH···O=C H-bonded dimers that have been considered as monomers. The dimerization energy be-comes 0.6 kcal/mol more negative than that using the naked dimer shown in Figure 5b, which is an indication of favorable cooperativity between the H-bonding and the π-hole interactions.

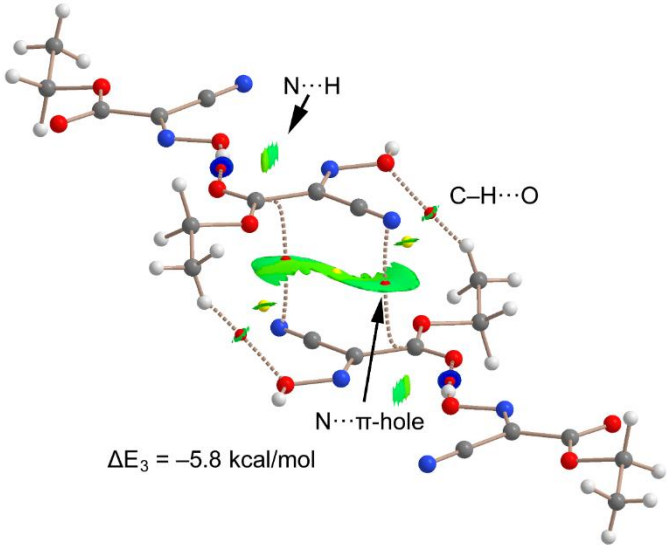

Figure 6. QTAIM/NCIPlot analysis of intermolecular bond CPs (red spheres), bond paths and RDG isosurfaces of a tetrameric assembly of the Oxyma (computed as a dimer of dimers).

4. Concluding Remarks

The X-ray structure of the orthorhombic polymorph of Oxyma has been revisited from a crystallographic point of view and computationally analyzed herein, showing interesting H-bonded and π-hole assemblies in the solid state. They were analyzed energetically using density functional theory (DFT) calculations, reduced density gradient isosurfaces and the topological analysis of bond critical points that was also used to estimate the contribution of each H-bond. In addition, energetically relevant N···π-hole interactions between the nitrile's N-atom and the carbonyl C-atom are described. Finally, favorable cooperativity effects have been studied, showing that the H-bonds reinforce the π-hole interactions. This effect is rationalized by the increase of the MEP value at the π-hole upon formation of the H-bond interaction, as revealed by the MEP study.

Supplementary Materials: The following are available online at https://www.mdpi.com/article/10.3390/cryst12060823/s1, Tables S1 and S2: Crystal data and structure refinement for orthorhombic polymorph of Oxyma. Figure S1: DSC of Oxyma bulk powder, Figure S2: TGA of Oxyma bulk powder. Figure S3: Comparative PXRD diffractograms between bulk Oxyma and simulated from the cif file, Table S3: Crystal data of forms of Oxyma reported in the CCDC compared with the orthorhombic revised structure, Section 4: checkCIF/PLATON report for reported WITSIB.

Author Contributions: Conceptualization, A.F. and R.P.; methodology, R.B., R.P., M.F.-B., D.d.S. and A.F.; validation, R.P., R.B.; formal analysis, R.B., R.P. and A.F.; investigation, A.F., R.P. and R.B.; resources, R.P. and A.F.; data curation, R.B.; writing—original draft preparation, A.F. and R.P.; writing—review and editing, A.F., R.B. and R.P.; supervision, A.F. and R.P.; project administration, A.F. and R.P.; funding acquisition, A.F. and R.P. All authors have read and agreed to the published version of the manuscript.

Funding: This research was funded by MICIU/AEI of Spain (project PID2020-115637GB-I00 FEDER funds).

Institutional Review Board Statement: Not applicable.

Informed Consent Statement: Not applicable.

Data Availability Statement: Data is contained within the article or Supplementary Material.

Acknowledgments: We thank the "centre de tecnologies de la informació" (CTI) at the University of the Balearic Islands for computational facilities.

Conflicts of Interest: The authors declare no conflict of interest.

References

1. Pimentel, G.C.; McClellan, A.L. *The Hydrogen Bond*; W.H. Freeman & Co.: San Francisco, CA, USA, 1960.
2. Desiraju, G.R.; Steiner, T. The Weak Hydrogen Bond. In *Structural Chemistry and Biology*; International Union of Crystallography, Oxford Science Publications: Oxford, UK, 1999.
3. Gilli, G.; Gilli, P. *The Nature of the Hydrogen Bond: Outline of a Comprehensive Hydrogen Bond Theory*; International Union of Crystallography, Oxford Science Publications: Oxford, UK, 2009.
4. Bauzá, A.; Mooibroek, T.J.; Frontera, A. The bright future of unconventional σ/π-hole interactions. *ChemPhysChem* **2015**, *16*, 2496–2517. [CrossRef] [PubMed]
5. Angarov, V.; Kozuch, S. On the σ, π and δ hole interactions: A molecular orbital overview. *New J. Chem.* **2018**, *42*, 1413–1422. [CrossRef]
6. Gao, L.; Zeng, Y.; Zhang, X.; Meng, L. Comparative studies on group III σ-hole and π-hole interactions. *J. Comput. Chem.* **2016**, *37*, 1321–1327. [CrossRef]
7. Bauza, A.; Mooibroek, T.J.; Frontera, A. Directionality of π-holes in nitro compounds. *Chem. Commun.* **2015**, *51*, 1491–1493. [CrossRef] [PubMed]
8. Murray, J.S.; Lane, P.; Clark, T.; Riley, K.E.; Politzer, P. σ-Holes, π-holes and electrostatically-driven interactions. *J. Mol. Model.* **2012**, *18*, 541–548. [CrossRef] [PubMed]
9. Zierkiewicz, W.; Michalczyk, M.; Scheiner, S. Noncovalent Bonds through Sigma and Pi-Hole Located on the Same Molecule. Guiding Principles and Comparisons. *Molecules* **2021**, *26*, 1740. [CrossRef]
10. Burgi, H.B.; Dunitz, J.D.; Shefter, E. Geometrical reaction coordinates. II. Nucleophilic addition to a carbonyl group. *J. Am. Chem. Soc.* **1973**, *95*, 5065–5067. [CrossRef]
11. Harder, M.; Kuhn, B.; Diederich, F. Efficient Stacking on Protein Amide Fragments. *Chemmedchem* **2013**, *8*, 397–404. [CrossRef] [PubMed]
12. Bartlett, G.J.; Choudhary, A.; Raines, R.T.; Woolfson, D.N. $n \rightarrow \pi^*$ interactions in proteins. *Nat. Chem. Biol.* **2010**, *6*, 615–620. [CrossRef] [PubMed]
13. Luxemburg Bio Technologies. Available online: https://www.luxembourg-bio.com/products/OxymaPure (accessed on 12 April 2022).
14. Subirós-Funosas, R.; Prohens, R.; Barbas, R.; El-Faham, A.; Albericio, F. Oxyma: An Efficient Additive for Peptide Synthesis to Replace the Benzotriazole-Based HOBt and HOAt with a Lower Risk of Explosion. *Chem. Eur. J.* **2009**, *15*, 9394–9403. [CrossRef] [PubMed]
15. Wehrstedt, K.D.; Wandrey, P.A.; Heitkamp, D. Explosive properties of 1-hydroxybenzotriazoles. *J. Hazard. Mater.* **2005**, *A126*, 1–7. [CrossRef] [PubMed]
16. El-Faham, A.; Al Marhoon, Z.; Abdel-Megeed, A.; Albericio, F. OxymaPure/DIC: An Efficient Reagent for the Synthesis of a Novel Series of 4-[2-(2-Acetylaminophenyl)-2-oxo-acetylamino] Benzoyl Amino Acid Ester Derivatives. *Molecules* **2013**, *18*, 14747–14759. [CrossRef] [PubMed]
17. Opalade, A.A.; Gomez-Garcia, C.J.; Gerasimchuk, N. New Route to Polynuclear Ni(II) and Cu(II) Complexes with Bridging Oxime Groups That Are Inaccessible by Conventional Preparations. *Cryst. Growth Des.* **2019**, *19*, 678–693. [CrossRef]
18. SADABS Bruker AXS.; Madison, Wisconsin, USA, 2004; *SAINT, Software Users Guide, Version 6.0*; Bruker Analytical X-ray Systems: Madison, WI, 1999. Sheldrick, G.M. SADABS v2.03; Area-Detector Absorption Correction; University of Göttingen: Germany, 1999. Saint, Version 7.60A.; Bruker AXS 2008; SADABS, V. 2008-1, 2008.
19. Sheldrick, G.M. A short history of SHELX. *Acta Crystallogr. Sect. A* **2008**, *64*, 112–122. [CrossRef]
20. Frisch, M.J.; Trucks, G.W.; Schlegel, H.B.; Scuseria, G.E.; Robb, M.A.; Cheeseman, J.R.; Scalmani, G.; Barone, V.; Petersson, G.A.; Nakatsuji, H.; et al. *Gaussian 16*; Revision B.01; Gaussian, Inc.: Wallingford, CT, USA, 2016.
21. Grimme, S.; Antony, J.; Ehrlich, S.; Krieg, H. A consistent and accurate ab initio parametrization of density functional dispersion correction (DFT-D) for the 94 elements H-Pu. *J. Chem. Phys.* **2010**, *132*, 154104–154118. [CrossRef]
22. Weigend, F. Accurate Coulomb-fitting basis sets for H to Rn. *Phys. Chem. Chem. Phys.* **2006**, *8*, 1057–1065. [CrossRef]
23. Boys, S.F.; Bernardi, F. The calculation of small molecular interactions by the differences of separate total energies. Some procedures with reduced errors. *J. Mol. Phys.* **1970**, *19*, 553–566.
24. Bader, R.F.W. A Bond Path: A Universal Indicator of Bonded Interactions. *J. Phys. Chem. A* **1998**, *102*, 7314–7323. [CrossRef]
25. Keith, T.A. *TK Gristmill Software*, version 13.05.06; AIMAll: Overland Park, KS, USA, 2013.
26. Contreras-García, J.; Johnson, E.R.; Keinan, S.; Chaudret, R.; Piquemal, J.-P.; Beratan, D.N.; Yang, W.J. NCIPLOT: A Program for Plotting Noncovalent Interaction Regions. *Chem. Theory Comput.* **2011**, *7*, 625–632. [CrossRef]
27. Johnson, E.R.; Keinan, S.; Mori-Sánchez, P.; Contreras-García, J.; Cohen, A.J.; Yang, W.J. Revealing noncovalent interactions. *Am. Chem. Soc.* **2010**, *132*, 6498–6506. [CrossRef]
28. Minacheva, L.K.; Raspertova, I.V.; Sliva, T.Y.; Lampeka, R.D. Crystal and Molecular Structures of 2-Cyano-2-Hydroxyiminoacetic Acid Ethyl Ester, HONC(CN)C(O)C2H5. *Russ. J. Coord. Chem.* **2000**, *26*, 226–228.
29. Emamian, S.; Lu, T.; Kruse, H.; Emamian, H. Exploring Nature and Predicting Strength of Hydrogen Bonds: A Correlation Analysis Between Atoms-in-Molecules Descriptors, Binding Energies, and Energy Components of Symmetry-Adapted Perturbation Theory. *J. Comput. Chem.* **2019**, *40*, 2868–2881. [CrossRef] [PubMed]